CHINESE OPTICS LETTERS

Vol. 22, No. 3 | March 2024

Stable ultraviolet ultrafast laser based on all-polarization-maintaining fiber femtosecond laser

Hao Tian (田 昊)[1,†], Zhe Zhu (朱 喆)[1,†], Wei Lin (林 巍)[1], Zihao Li (李子豪)[1], Junpeng Wen (温俊鹏)[1], Hao Xiu (修 昊)[1], Yiheng Fan (范怡衡)[1], Chiyi Wei (韦池一)[1], Xiaoming Wei (韦小明)[1*], and Zhongmin Yang (杨中民)[1,2**]

[1] School of Physics and Optoelectronics; State Key Laboratory of Luminescent Materials and Devices, Guangdong Engineering Technology Research and Development Center of Special Optical Fiber Materials and Devices, Guangdong Provincial Key Laboratory of Fiber Laser Materials and Applied Techniques, South China University of Technology, Guangzhou 510640, China

[2] Research Institute of Future Technology, South China Normal University, Guangzhou 510006, China

[†]These authors contributed equally to this work.

*Corresponding author: xmwei@scut.edu.cn

**Corresponding author: yangzm@scut.edu.cn

Received August 6, 2023 | Accepted November 29, 2023 | Posted Online March 22, 2024

We report a high-stability ultrafast ultraviolet (UV) laser source at 352 nm by exploring an all-fiber, all-polarization-maintaining (all-PM), Yb-doped femtosecond fiber laser at 1060 nm. The output power, pulse width, and optical spectrum width of the fiber laser are 6 W, 244 fs, and 17.5 nm, respectively. The UV ultrashort pulses at a repetition rate of 28.9 MHz are generated by leveraging single-pass second-harmonic generation in a 1.3-mm-long BiB_3O_6 (BIBO) and sum frequency generation in a 5.1-mm-long BIBO. The maximum UV output power is 596 mW. The root mean square error of the output power of UV pulses is 0.54%. This laser, with promising stability, is expected to be a nice source for frontier applications in the UV wavelength window.

Keywords: all-polarization-maintaining fiber; ultrafast fiber laser; UV laser.

DOI: 10.3788/COL202422.031404

1. Introduction

Ultrafast ultraviolet (UV) sources possess high peak power as well as high photon energy. Thus, they prevail in a wealth of applications, such as ophthalmology[1], frontier biological research[2], and high-end electron diffraction[3]. Particularly, in the field of laser machining, due to their high single-photon energy, UV pulses directly break the chemical bonds of the material[4–6], and ablate the material within the irradiated spot quickly without affecting the surrounding area. In this regard, they facilitate high-quality micromachining by maximumly suppressing heat-induced deformation or damage[7–9].

By far, ultrafast UV pulses are mostly generated by parametric oscillation[10,11] and nonlinear frequency conversion (NFC), mainly using near-infrared (NIR) solid-state lasers. Notably, for the process of NFC occurring in nonlinear optical crystals, such as LiB_3O_5 (LBO)[12,13], β-BaB_2O_4 (BBO)[14,15], and BiB_3O_6 (BIBO)[16,17], the reliability is largely determined by the driven pulse, thereby requiring ultrafast pump lasers with high stabilities of power and polarization. In comparison to solid-state lasers with relatively large volume, complex structure, and inconvenient heat dissipation, fiber lasers are featured by a small footprint, good robustness, high stability, low cost, and excellent heat management. Also, benefiting from the use of large-mode-area fibers, e.g., chirally coupled-core fiber[18] and large-pitch fiber[19], the scalabilities of both average power and pulse energy are fairly satisfying.

Recently, the proposal of a figure-9 configuration with all-polarization-maintaining (all-PM) architecture has allowed one to further upgrade the performance of mode-locked fiber lasers[20]. In contrast to the mode-locking strategies using semiconductor saturable absorber mirrors (SESAMs)[21] and nonlinear polarization evolution (NPE) technology, this scheme prevents thermal damage and simultaneously has fast-response saturable absorption in all-PM format. Based on such promising pulsed laser sources, scalabilities of pulse energies to 3 nJ[22] and 141 nJ[23] have been successfully demonstrated at distinctive wavelengths.

Here, we report a high-stability ultrafast UV source based on 1.0-μm all-PM figure-9 mode-locked fiber laser. Driven by 1060-nm femtosecond pulses with 6-W average power, second-harmonic generation (SHG) and sum frequency generation (SFG) are implemented by using two BIBO crystals. The built figure-9-based laser system delivers 596-mW ultrafast UV pulses operating at a 28.9 MHz repetition rate, and exhibits good

power stability characterized by a root-mean-square error (RMSE) of 0.54%.

2. Experimental Setup

The setup of the all-PM fiber ultrafast laser system is portrayed in Fig. 1. The fiber laser system consists of a seed, a stretcher, a preamplifier, and a main amplifier. The seed is an all-PM figure-9 fiber laser wherein a nonlinear amplifying loop mirror (NALM) acts as the artificial mode locker in which the dispersion is managed. A Yb-doped fiber (YDF, INO FaseFBR Yb 401-PM) with a length of 50 cm and a single-mode laser diode (SM-LD, 976 nm wavelength) as the pump source through a wavelength division multiplexer (WDM) are used. A chirped fiber Bragg grating (CFBG, TeraXion, 1064 nm center

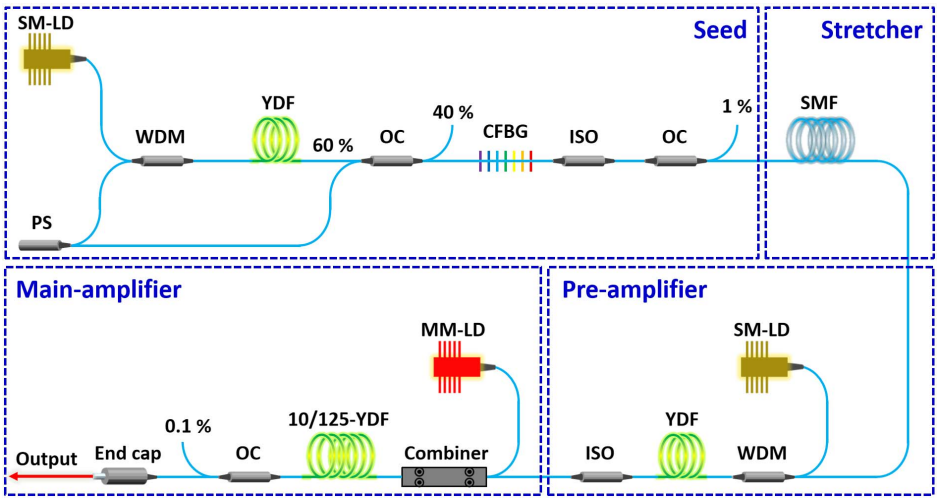

Fig. 1. Sketch of the all-PM fiber ultrafast laser system. SM-LD, single-mode laser diode; WDM, wavelength division multiplexer; YDF, Yb-doped fiber; OC, optical coupler; PS, phase shifter; CFBG, chirped fiber Bragg grating; ISO, isolator; MM-LD, multimode laser diode.

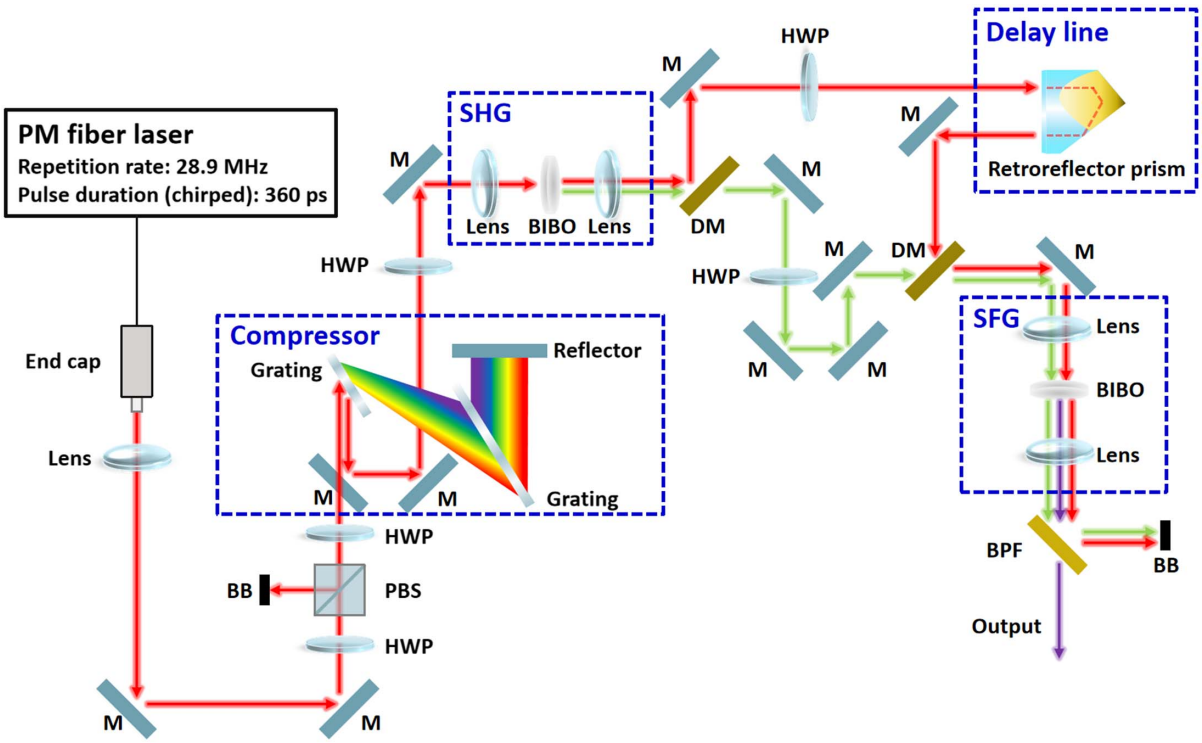

Fig. 2. Schematic diagram of UV pulse generation. M, mirror; HWP, half-wave plate; PBS, polarization beam splitter; BB, beam barrier; DM, dichroic mirror; BPF, bandpass filter.

wavelength, 25 nm reflection bandwidth at 3-dB, 25% reflectivity, 0.25 ps/nm) is used to provide anomalous dispersion, and fine adjustment of intracavity dispersion is fulfilled by further controlling the cavity length. A phase shifter (PS) is applied to provide $\pi/2$ nonreciprocal phase shift for robust mode locking. In the asymmetric structure of NALM, 60% port of the optical coupler (OC) is connected with the segment of YDF, ensuring the self-starting of the laser and the accessibility of high output power. The output port of the OC with a ratio of ∼40% is spliced with an angled physical contact (APC) connector to prevent backreflection. In addition, the seed also includes an isolator to guarantee its long-term stability and a 1/99 OC to monitor the working status. In the stretcher, the pulse is prechirped to about 360 ps through a 500-m-long single-mode fiber (SMF, PM980). Then, the stretched pulse is sent to the preamplifier, in which a 1-m-long YDF (INO FaseFBR Yb 401-PM) is core-pumped via an SM-LD (976 nm wavelength, 680 mW maximum output power). In the main amplifier, a 3.5-m-long double-clad Yb-doped fiber (Coherent PLMA-YDF-10/125-M) is chosen as the gain medium, pumped by a multimode laser diode (MM-LD) through a combiner. After the gain fiber, a 1/99 OC is used to monitor the laser output and is connected to the end cap for the final output.

For generating UV pulses, the experimental setup of NFC is illustrated in Fig. 2. It comprises a compressor and modules for SHG and SFG. Since the 1.0-μm pulsed laser output from the end cap has a certain beam divergence, a lens ($f = 30$ mm) is used to collimate the beam; subsequently, two mirrors are employed to adjust the propagation direction of the beam. Because the transmission efficiency of the grating is polarization-dependent, a polarization beam splitter (PBS) and two half-wave plates (HWPs) are utilized to linearly polarize the output laser, while the residual part is blocked by a beam barrier (BB). After adjusting the polarization orientation of the incident beam, the pulse is compressed by a grating pair (LightSmyth, 1060 ± 20 nm wavelength range, 1600 lines/mm group density, 58° ± 1° maximum diffraction angle, ≥94% maximum diffraction efficiency). Prior to the SHG module, another HWP is placed to readjust the polarization. Here, BIBOs are employed to perform NFC because of the high nonlinear coefficient (∼3.34 pm/V) and high damage threshold. A pair of double-glued achromatic lenses ($f = 50$ mm) are used to converge and collimate the beam, and the first BIBO crystal [CASTECH, YZ optical plane, type-I (e + e = o), $d = 1.3$ mm, $\theta = 168.5°$, $\varphi = 90°$] is placed in the common focus of the two lenses to generate a green laser at near 530 nm wavelength. The group velocity dispersion has to be considered for pulse-pumped SFG, and the resultant temporal walk-off caused by group velocity mismatch may degrade the pulse quality. To mitigate this, the length of the crystal in use should be relatively thin. After SHG, the NIR 1.0-μm laser beam is separated from the green laser beam by a dichroic mirror (DM, Thorlabs DMSP650, short-wave pass, long-wave reflection). To temporally overlap the second-harmonic and fundamental pulses, an optical delay line is constructed in the NIR arm via exploiting a retroreflector prism (Thorlabs PS976M-M01B). The two-color pulses are further combined through a DM (the same model as the previous one). In the SFG part, the first lens is an achromatic doublet ($f = 100$ mm), which is used to gather two signal beams. The second BIBO crystal [CASTECH, YZ optical plane, type-I (e + e = o), $d = 5.1$ mm, $\theta = 142°$, $\varphi = 90°$] used for SFG is placed at the beam waist. The second lens used for alignment is a fused silica UV antireflection lens ($f = 100$ mm). Finally, a short-pass filter is used to filter out the residual green and NIR laser, resulting in ultrafast UV pulse output. The key parameters of the experimental setup are provided in Table 1.

Table 1. Key Parameters of the Experimental Setup.

Part	Parameter	Value
Seed	CFBG's second-order dispersion	0.25 ps/nm
	CFBG's reflectivity	25%
	Cavity length	6.5 m
	Gain fiber length	50 cm
Stretcher	Fiber length	500 m
Preamplifier	Gain fiber length	1 m
Main amplifier	Gain fiber length	3.5 m
Compressor	Grating's group density	1600 lines/mm
	Grating's maximum diffraction angle	58° ± 1°
	Grating's maximum diffraction efficiency	≥94%
SHG	Lens's focal length	50 mm
	BIBO's length	1.3 mm
	BIBO θ	168.5°
	BIBO φ	90°
SFG	Lens's focal length	100 mm
	BIBO's length	5.1 mm
	BIBO θ	142°
	BIBO φ	90°

3. Results and Discussion

As a key unit to assure high stability of the pulsed laser system, the all-PM dispersion managed figure-9 fiber laser is characterized at a pump power of ∼100 mW, as seen in Fig. 3.

Figure 3(a) presents the optical spectrum of the laser measured, the results of which were measured by a commercial optical spectrum analyzer (OSA, Yokogawa AQ6370D), indicating a center wavelength of 1060 nm and a 3-dB bandwidth of 18.3 nm. The hump near 1030 nm is caused by amplified spontaneous emission (ASE), and its peak intensity is about 24 dB

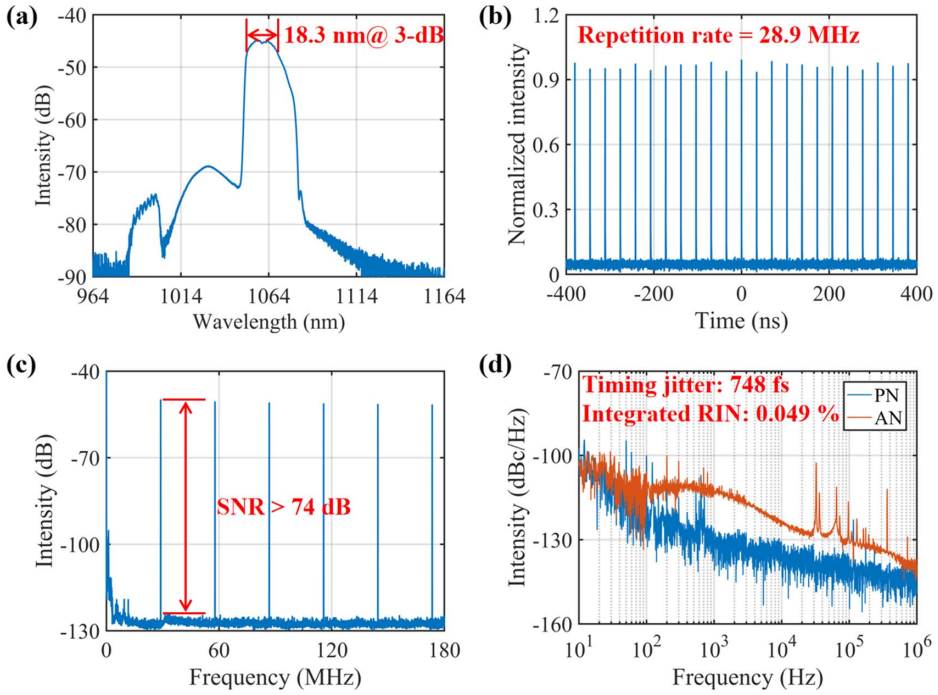

Fig. 3. Performance of the figure-9 mode-locked fiber laser. (a) Optical spectrum; (b) oscilloscopic trace; (c) RF spectrum; (d) PN and RIN.

lower than that of the signal so that it merely affects the subsequent power amplification. Figure 3(b) shows the oscilloscopic trace of the mode-locked pulse train at a repetition rate of 28.9 MHz. Figure 3(c) depicts the corresponding radio-frequency (RF) spectrum; the signal-to-noise ratio (SNR) is manifested to be greater than 74 dB. The phase noise (PN) and the relative intensity noise (RIN) are shown in Fig. 3(d), and the timing jitter and integrated RIN are 748 fs and 0.049%, respectively. The low-noise performance can mainly be contributed by the advantages of the all-PM architecture.

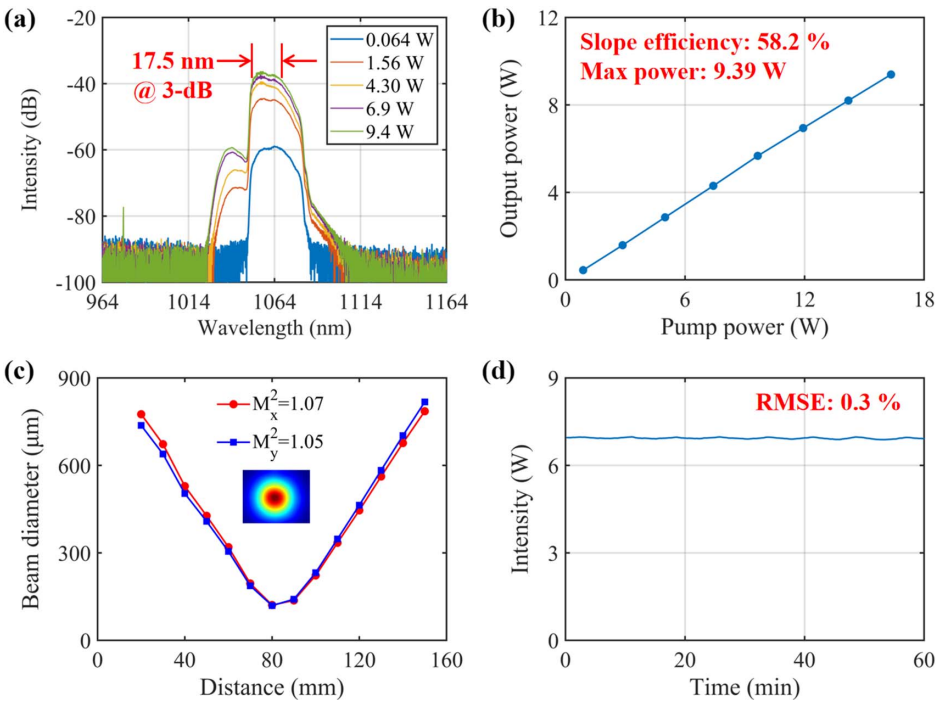

Fig. 4. Performance of the 1.0-μm high-power all-PM Yb-doped ultrafast fiber laser. (a) Optical spectrum measured at 1% port of OC; (b) output power of the main amplifier varying against launched pump power; (c) M^2 measurement of the amplified laser beam; (d) power stability at 6.9 W in 1-h test.

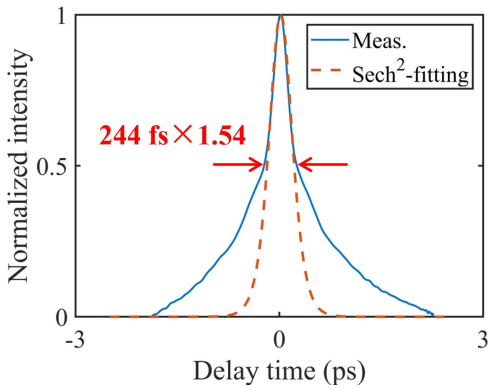

Fig. 5. Autocorrelation trace of the 1.0-μm pulse after the compressor.

Given that power amplification of the seed is required prior to NFC, output characteristics of the 1.0-μm high-power all-PM Yb-doped ultrafast fiber laser are summarized in Fig. 4. Figure 4(a) shows the spectrum of the laser under different pump powers. As seen, nonlinear spectral broadening that mainly contributes to self-phase modulation is well suppressed after prechirping. The accompanying ASE is considerably weak, rendering a spectral SNR of >20 dB. It should be noted that there exist fine modulation structures on the optical spectrum, which can be ascribed to several ingredients, like nonlinearity[24] and multimodal interference. As seen in Fig. 4(b), the slope efficiency of the amplification is 58.2% as the output power increases to its maximum of 9.39 W. Figure 4(c) depicts the beam quality measurement, and the M^2 of the laser beam is less than 1.07. The final 1.0-μm all-PM fiber ultrafast laser system exhibits an output power RMSE of only 0.3% within 1 h, recorded in Fig. 4(d). These results again highlight the advantage of the figure-9 all-PM fiber design. The pulse duration of the amplified pulses is compressed from 360 ps to 244 fs (assuming a hyperbolic-secant pulse shape), as shown in Fig. 5, which exhibits a pedestal due to the residual nonlinear chirp introduced by a 500-m-long SMF in the stretcher and the nonlinear phase shift accumulated during the amplification.

After pulse compression, the femtosecond pulses are launched to generate 530-nm pulses via SHG; the results are given in Fig. 6. Figure 6(a) depicts the output power of the SHG pulses and corresponding SHG efficiency as a function of the input power. As the input power of the fundamental laser increases, the power of the SHG component gradually increases, reaching an output power up to 2.28 W, i.e., a conversion efficiency of 38%. It should be pointed out that the efficiency of the SHG can be further improved by optimizing the pulse pedestal. To do this, PM-CFBG with lower higher-order dispersion is promising. According to the efficiency of the SHG, a saturation effect manifests itself as the input power of the fundamental pulse exceeds 3 W. The beam profile is well maintained after SHG, as can be visualized in the inset in Fig. 6(a). Figure 6(b) shows the optical spectrum of the SHG pulses captured by another OSA (Ocean Optics HR2000 + ES), wherein a center wavelength of 530 nm and a 3-dB bandwidth of about 2 nm are recognized. Benefiting from the 1.0-μm all-PM fiber laser system, the generated SHG pulses exhibit an output power RMSE of only 0.35% within 1 h, as shown in Fig. 6(c).

Finally, the SFG using the fundamental and SHG laser beams is carried out to generate UV pulses. The output power and

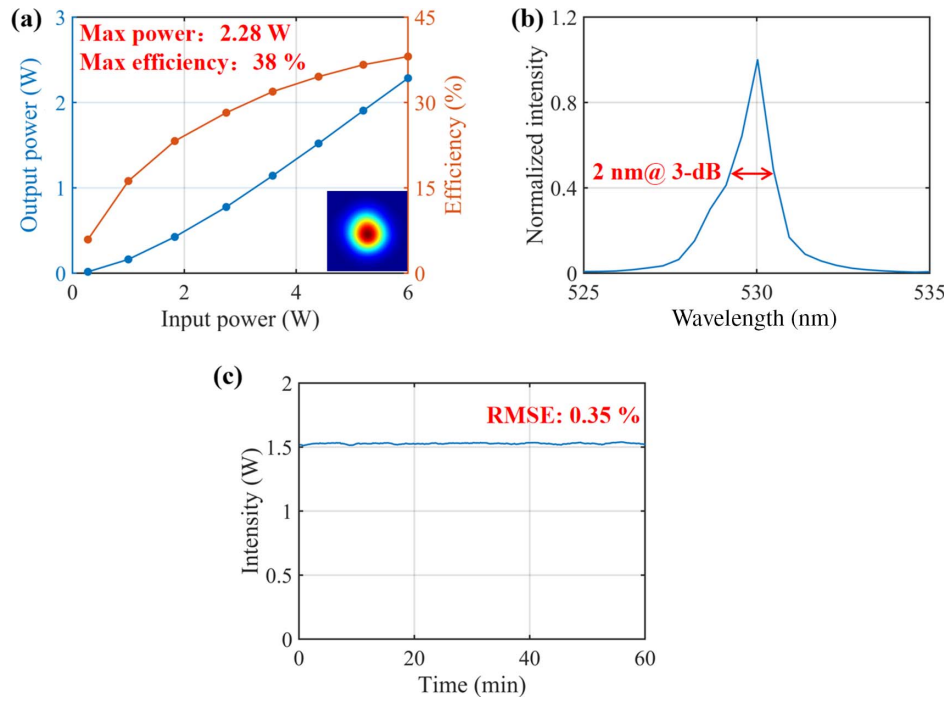

Fig. 6. Performance of the SHG. (a) Output power of the second-harmonic component and corresponding efficiency with varying input powers; (b) optical spectrum; (c) power stability of SHG within 1 h.

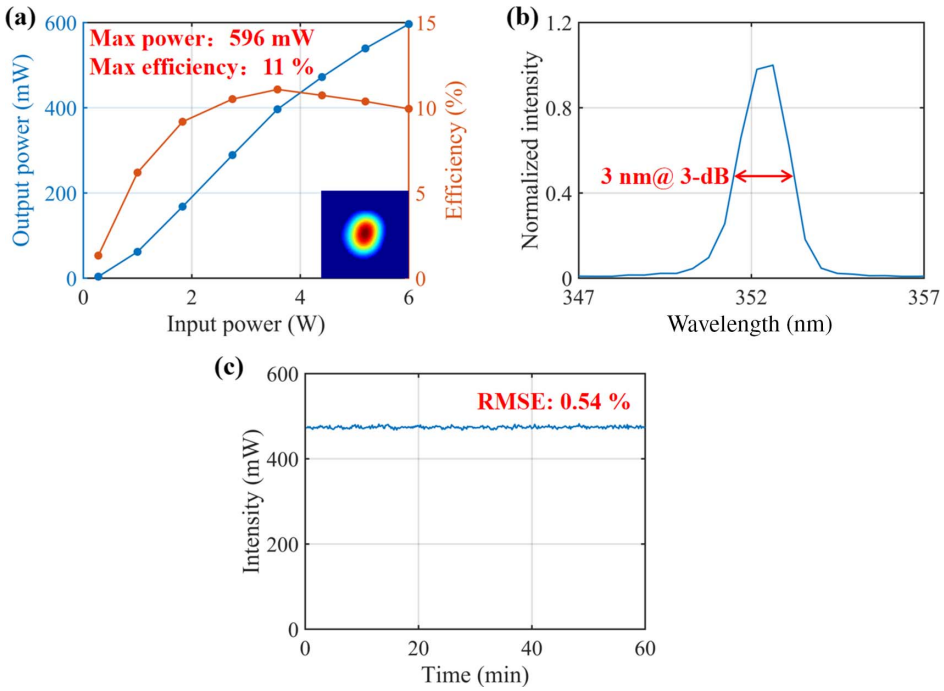

Fig. 7. Performance of the SFG. (a) Variation of the SFG power and efficiency with the input power of fundamental light; (b) optical spectrum; (c) power stability of SFG within 1 h.

relevant conversion efficiency of the SFG versus the input power of 1.0-μm pulsed laser are shown in Fig. 7(a). The maximum output power at the UV wavelength reaches 596 mW for an input power of 6 W. The maximum third-harmonic generation (THG) efficiency is about 11% for an input power 3.58 W. It is saturated when the average power of the fundamental source exceeds 1.6 W, and THG efficiency slightly declines when the power of the fundamental source exceeds 3.6 W. Figure 7(b) depicts the optical spectrum of the UV pulses, indicating a center wavelength of 352 nm and a 3-dB bandwidth of about 3 nm. The achieved bandwidth implies a transform-limited pulse duration of <50 fs. However, in practice, the THG pulses are typically broadened to a duration of a subpicosecond due to the presence of the walk-off effect and group velocity dispersion of the nonlinear crystal[17]. Within 1 h, the ultrafast UV laser exhibits an output power RMSE of only 0.54% [see Fig. 7(c)], implying a good power stability inherited from the all-PM fiber laser system. Please note that, as evidenced by relatively narrow bandwidths of the pulses of SHG and SFG, there are limitations on phase-matching bandwidth of the nonlinear crystals. Primary performance metrics of the laser system are summarized in Table 2.

Table 2. Primary Performance Metrics of the Laser System.

Process	Parameter	Value
Fundamental source	Output average power	6 W
	3-dB spectral width	17.5 nm
	Center wavelength	1060 nm
	Repetition rate	28.9 MHz
	Pulse duration	244 × 1.54 fs
	RMSE	0.3%
SHG	Output average power	2.28 W
	Maximum efficiency	38%
	Center wavelength	530 nm
	RMSE	0.35%
THG	Output average power	596 mW
	Maximum efficiency	11%
	Center wavelength	352 nm
	RMSE	0.54%

4. Conclusion

In this paper, we have experimentally investigated a high-stability ultrafast UV laser source at 352 nm, based on an all-PM Yb-doped ultrafast fiber laser at 1060 nm. The seed laser at 1.0 μm was designed with all-PM fibers in a figure-9 configuration. The high-power fiber amplification system was also constructed by all-PM fiber components. After the nonlinear processes of SHG and subsequent SFG, the UV pulses with a center wavelength of 352 nm were obtained, with the output

power reaching 596 mW. Taking full advantage of the good stability of the all-fiber all-PM system, the RMSE of the output power in a 1-h test without an additional feedback loop is as low as 0.54%. We believe that this UV ultrafast laser source will have wide application prospects in laser microprocessing, the frontiers of biological research, and other scientific fields.

Acknowledgements

This work was partially supported by the National Natural Science Foundation of China (NSFC) (Nos. 62375087, 12374304, U1609219, and 62235014), the NSFC Development of National Major Scientific Research Instrument (No. 61927816), the Mobility Programme of the Sino-German (No. M-0296), the Introduced Innovative Team Project of Guangdong Pearl River Talents Program (No. 2021ZT09Z109), the Natural Science Foundation of Guangdong Province (No. 2021B1515020074), and the Science and Technology Project of Guangdong (No. 2020B1212060002).

References

1. Q. Ren, G. Simon, J. Legeais, *et al.*, "Ultraviolet solid-state laser (213-nm) photorefractive keratectomy: *in vivo* study," Ophthalmology **101**, 883 (1994).
2. A. Steube, T. Schenk, A. Tretyakov, *et al.*, "High-intensity UV laser ChIP-seq for the study of protein-DNA interactions in living cells," Nat. Commun. **8**, 1303 (2017).
3. M. Z. Mo, Z. Chen, R. K. Li, *et al.*, "Heterogeneous to homogeneous melting transition visualized with ultrafast electron diffraction," Science **360**, 1451 (2018).
4. R. Srinivasan and V. Mayne-Banton, "Self-developing photoetching of poly-(ethylene terephthalate) films by far-ultraviolet excimer laser radiation," Appl. Phys. Lett **41**, 576 (1982).
5. K. C. Yung, D. W. Zeng, and T. M. Yue, "XPS investigation of Upilex-S polyimide ablated by 355 nm Nd:YAG laser irradiation," Appl. Surf. Sci. **173**, 193 (2001).
6. W. J. Lee, Y. S. Lee, S. K. Rha, *et al.*, "Adhesion and interface chemical reactions of Cu/polyimide and Cu/TiN by XPS," Appl. Surf. Sci. **205**, 128 (2002).
7. R. R. Gattass and E. Mazur, "Femtosecond laser micromachining in transparent materials," Nat. Photon. **2**, 219 (2008).
8. F. Zhang, J. Duan, X. Y. Zeng, *et al.*, "Drilling blind holes on multi-layer FPC board with a 355 nm UV laser," Infrared Laser Eng. **39**, 143 (2010).
9. C. Kerse, H. Kalaycıoğlu, P. Elahi, *et al.*, "Ablation-cooled material removal with ultrafast bursts of pulses," Nature **537**, 84 (2016).
10. W. R. Bosenberg, A. Drobshoff, J. I. Alexander, *et al.*, "93% pump depletion, 3.5-W continuous-wave, singly resonant optical parametric oscillator," Opt. Lett. **21**, 1336 (1996).
11. L. E. Myers, W. R. Bosenberg, R. C. Eckardt, *et al.*, "Multigrating quasi-phase-matched optical parametric oscillator in periodically poled $LiNbO_3$," Opt. Lett. **21**, 591 (1996).
12. C. Chen, Y. Wu, A. Jiang, *et al.*, "New nonlinear-optical crystal: LiB_3O_5," J. Opt. Soc. Am. B **6**, 616 (1989).
13. S. Lin, Z. Sun, B. Wu, *et al.*, "The nonlinear optical characteristics of a LiB_3O_5 crystal," J. Appl. Phys. **67**, 634 (1990).
14. C. Chen, W. Bochard, and J. Aidong, "A new-type ultraviolet SHG crystal β-BaB_2O_4," Sci. China, Ser. B **28**, 235 (1985).
15. D. C. Edelstein, E. S. Wachman, L. K. Cheng, *et al.*, "Femtosecond ultraviolet pulse generation in β-BaB_2O_4," Appl. Phys. Lett **52**, 2211 (1988).
16. S. C. Kumar, E. S. Bautista, and M. Ebrahim-Zadeh, "Stable, high-power, Yb-fiber-based, picosecond ultraviolet generation at 355 nm using BiB_3O_6," Opt. Lett. **40**, 403 (2015).
17. N. Apurv Chaitanya, A. Aadhi, M. V. Jabir, *et al.*, "High-power, high-repetition-rate, Yb-fiber laser based femtosecond source at 355 nm," Opt. Lett. **40**, 4269 (2015).
18. L. Chi-Hung, G. Chang, N. Litchinitser, *et al.*, "Chirally coupled core fibers at 1550-nm and 1064-nm for effectively single-mode core size scaling," in *Conference on Lasers and Electro-Optics* (2007), p. 1.
19. J. Limpert, F. Stutzki, F. Jansen, *et al.*, "Yb-doped large-pitch fibres: effective single-mode operation based on higher-order mode delocalisation," Light Sci. Appl. **1**, e8 (2012).
20. W. Hänsel, H. Hoogland, M. Giunta, *et al.*, "All polarization-maintaining fiber laser architecture for robust femtosecond pulse generation," in *Exploring the World with the Laser: Dedicated to Theodor Hänsch on his 75th Birthday*, D. Meschede, T. Udem, and T. Esslinger, eds. (Springer International Publishing, 2018), p. 331.
21. U. Keller, K. J. Weingarten, F. X. Kartner, *et al.*, "Semiconductor saturable absorber mirrors (SESAM's) for femtosecond to nanosecond pulse generation in solid-state lasers," IEEE J. Sel. Top. Quantum Electron **2**, 435 (1996).
22. F. Chen, Q. Hao, and H. Zeng, "Optimization of an NALM mode-locked all-PM Er:fiber laser system," IEEE Photon. Technol. Lett **29**, 2119 (2017).
23. Y. Li, N. Kuse, A. Rolland, *et al.*, "Low noise, self-referenced all polarization maintaining ytterbium fiber laser frequency comb," Opt. Express **25**, 18017 (2017).
24. J. Wu, Z. Liang, W. Lin, *et al.*, "All-fiber high-power 3 GHz ultrafast laser system at 2.0 μm," J. Lightwave Technol. **41**, 1559 (2023).